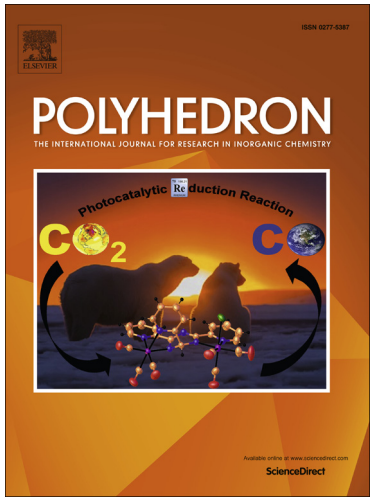

Experimental and theoretical studies on Cu(II) complex of N,N'-disalicylidene-2,3-diaminopyridine ligand reveals indirect evidence for DNA intercalation

Abdulkadir Kocak, Ozlem Faiz, Hakan Yilmaz, Omer Andac

PII: S0277-5387(15)00723-8
DOI: http://dx.doi.org/10.1016/j.poly.2015.11.037
Reference: POLY 11682

To appear in: *Polyhedron*

Received Date: 21 September 2015
Accepted Date: 19 November 2015

Please cite this article as: A. Kocak, O. Faiz, H. Yilmaz, O. Andac, Experimental and theoretical studies on Cu(II) complex of N,N'-disalicylidene-2,3-diaminopyridine ligand reveals indirect evidence for DNA intercalation, *Polyhedron* (2015), doi: http://dx.doi.org/10.1016/j.poly.2015.11.037

Experimental and theoretical studies on Cu(II) complex of N,N'-disalicylidene-2,3-diaminopyridine ligand reveals indirect evidence for DNA intercalation

Abdulkadir Kocak[a,*], Ozlem Faiz[b], Hakan Yilmaz[c], and Omer Andac[c]

[a] *Department of Chemistry, Gebze Technical University, 41400 Kocaeli, Turkey*
[b] *Department of Chemistry, Recep Tayyip Erdogan University, 53100 Rize, Turkey.*
[c] *Department of Chemistry, Ondokuz Mayis University, 55200 Samsun, Turkey.*

Abstract

A potential DNA intercalating Cu(II) complex ([CuL]) of the N,N'-disalicylidene-2,3-diaminopyridine ligand (H_2L; dianion=L^{2-}) has been synthesized and characterized. The photophysical and the DNA binding behaviors of the neutral [CuL] have been investigated both experimentally and theoretically. Experimental studies reveal that the [CuL] has a quite strong interaction with the Calf Thymus DNA (ctDNA) with $K_b = (1.53 \pm 0.48) \times 10^6$. Experimental bathochromism of 4 nm and hypochromism of ~50% on the absorption band of the [CuL] at 408 nm by intercalation were reproduced by calculations. The competitive displacement experiments were carried out using methylene blue (MB) and ethidium bromide (EB). Viscosity measurements totally supported the intercalative interaction. Quantum mechanical calculations using time dependent density functional theory

* Corresponding author: Phone: +90 262 605 3084; Fax: +90 262 605 3005; E-Mail: kocak@gtu.edu.tr

(TDDFT) coupled with polarizable continuum model were carried out in the proposed dimer of deoxyguanosine-monophosphate-deoxycytidine, $d(GpC)_2$, intercalation pocket. The calculations qualitatively confirmed the intercalative binding. In addition, vertical excitation calculations showed that electronic excitations of H_2L are affected by the environment and Cu^{2+} ion. The electronic transitions of the [CuL] are involved in mostly π-π^* transitions but includes significant contribution from the charge transfer. According to the calculations, the electronic spectrum of the [CuL] is sensitive to the DNA intercalation because of the π-π stacking interaction between the DNA base pairs and aromatic rings of the [CuL].

Keywords

DNA intercalation, Schiff base, salphen, absorption, density functional theory, π-π stacking.

1. Introduction

Attaching small molecules to DNA with high affinity has been a goal of drug design in the recent years due to the possibility of developing anticancer and antibiotics drugs since DNA is ultimately responsible for all the cell functions [1]. Comparing to proteins, studies on DNA as a drug target are still very limited as opposed to well-known structure of DNA [1]. The attachment (and thus disfunctioning of the DNA) can be done by a) irreversible covalent binding or metal coordination to the bases b) reversible non-covalent as minor/major groove bindings c) intercalation and d) sugar-phosphate (phosphodiester) backbone binding [2-4].

Salen and salphen type ligands and their corresponding metal complexes, apart from their outstanding applications such as efficient molecular sensors related to fluorescence detections of biologically common ions [5-13] and as on-off light switch behaviors by multi-fold fluorescence enhancement or quenching upon saturation [14-25], are excellent DNA interacting systems. The findings of the literature studies on metal complexes of salen and salphen type ligands such as Al [26], V [27], Mn [28-31], Fe [32, 33], Co [30, 34], Ni [2,5,6,11] Cu [27, 30, 35, 36] and Zn [27] show that the interaction depends on the nature of the ligand and coordination around the metal ion [37].

The interaction between the DNA and small metal complexes can be measured by direct methods such as X-ray crystallography and NMR techniques or by indirect methods such as electronic absorption, fluorescence spectroscopy, viscosity measurements and circular dichroism [3, 38]. Since computational treatment of the interaction phenomenon can provide useful

information at the atomistic level, there have been numerous computational efforts on both large or small scale [39, 40]. These include molecular dynamics (MD) simulations of small molecule – DNA oligomer interaction, performed for imaging particularly groove binding modes [41-44]; hybrid quantum mechanics (QM) and molecular mechanics (MM) calculations for modeling both intercalative and groove binding modes of the ligand - DNA oligomers [38, 45, 46]; or pure QM calculation including only the DNA dimers at the intercalation pocket [37, 45, 47, 48].

A new salphen type Schiff base, N,N'-disalicylidene-2,3-diaminopyridine (H_2L), was first prepared and characterized by Bosner and co-workers [49]. Later, Atakol [50] et al. successfully crystalized neutral Cu(II) complex ([CuL]) of dianion of H_2L, but it was never characterized in detail until recently [51-53]. Asadi et al. [53] characterized the [CuL] complex (in methanol) using UV-Vis, FT-IR and H-NMR techniques. The potential DNA binding features and photophysical behaviors have never been investigated (Figure 1).

Here, we report experimental studies of the [CuL] to explore DNA intercalation properties along with theoretical calculations on both [CuL] and its insertion to double stranded DNA dimer via intercalation.

2. Experimental and Computational Methods

2.1 Materials

The 2-3-diaminopyridine, salicylaldehyde, and solvents (DMF and EtOH) were purchased from Sigma-Aldrich and used without further purification. For

the intercalation experiments, Calf Thymus DNA (ctDNA), Ethidium Bromide (EB), Methylene Blue (MB) and all the solvents and reagents used to prepare buffer were purchased from the same commercial supplier (Sigma-Aldrich).

Single crystal x-ray data were collected using STOE X-AREA diffractometer at 293±2 K using Mo Kα radiation (λ=0,71073Å). The structures were solved by direct methods using SHELXS-97 and refined by a full-matrix least-squares procedure using the program SHELXL-97[54, 55].

ESI-MS spectrum was taken by LC/MS (HPLC unit: Agilent 1260 Infinity Series, TOF-MS unit: Agilent 6230), at Central Research Laboratory, Giresun University.

The ctDNA binding studies of [CuL] along with its competitive displacement experiments with MB and EB were carried out by electronic spectroscopy on Shimadzu UV 1601. Viscosity measurements were performed at 25 °C on Ostwald-type viscometer.

The DFT calculations were carried out using Gaussian 09 (G09) Rev. D01 software package [56].

2.2 Synthesis and Characterization

2.2.1 H_2L Ligand

The procedure for the synthesis of the H_2L was described elsewhere [52]. Briefly, 2,3-diaminopyridine (in EtOH) was treated with hot solution of salicylaldehyde (in EtOH), with the ratio of 1:2 for 3-4 h at 50 °C. Upon cooling, the solid orange product was immediately filtered, washed with ethanol, ether, and dried in air.

2.2.2 [CuL]

For the synthesis of the [CuL], the H_2L ligand was simply mixed with $Cu(CH_3COO)_2$ (1:1 ratio) in an abundant solvent (EtOH) environment and stirred ~1 hour in hot solvent bath. Hot solution was filtered and cooled for crystallization.

Elemental Analysis: [CuL] with empirical formula of $C_{19}H_{13}CuN_3O_2$ Observed: 59.83% C, 3.77% H, and 10.93% N. Calculated ([CuL]): 60.23% C, 3.46% H and 11.09% N.

ESI-MS of [CuL]: The characteristic molecular ion peak of [CuL] was observed at m/z=379 (100%), confirming the formation of the [CuL] complex. The relative abundance of the ^{65}Cu isotopomer peak at m/z=381 also supports the structure. (Figure S1)

XRD of H_2L and [CuL]: The structure of the [CuL] complex confirms the square planar geometry while the H_2L ligand is non-planar. Selected bond distances and dihedral angles for the H_2L ligand and [CuL] complex are given in Table 1. The crystallographic data are summarized in Table S1. Both H_2L ligand and [CuL] complex adopt monoclinic $P_{21/c}$ space group. The structures will be discussed in detail in the results section.

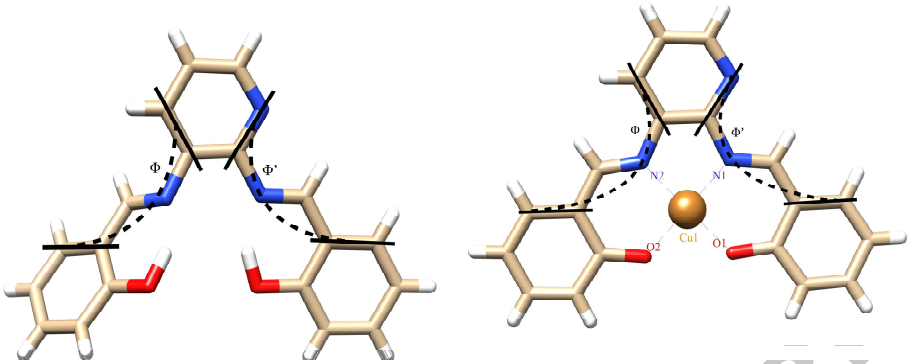

Figure 1. Molecular structures of H_2L (left) and [CuL] (right) from the X-ray crystallographic data. The bond distances and dihedral angles of the labeling are discussed in section 3.1.

2.3 DNA Interaction Experiments

The ratio of observed absorption of ctDNA at 260 and 280 nm was A_{260}/A_{280} = 1.9, indicating sufficient purity of the DNA (devoid of proteins). For the binding studies, 500 µM stock solution of ctDNA in 5mM the tris(hydroxymethyl)aminomethane (Tris)/HCl buffer with pH=7.2 and I=0.1 M (NaCl) was kept in the dark at 4 °C and used within 2 days of preparation. The concentration of the DNA in monomer units was determined using the molar extinction coefficient ($\varepsilon_{260} = 6600\, L.mol^{-1}cm^{-1}$) at 260 nm [57]. Due to the low solubility in water, the stock solutions of [CuL] (1 mM) were first prepared in DMF (Sigma Aldrich, purity >99%) and then diluted to 15 µM with the Tris buffer, in which the DMF content was negligible (5% DMF in the Tris buffer). The isolated [CuL] in the solvent mixture was verified for no shift on the spectra for 10 minutes, which has been used as standard incubation time for the DNA binding experiments.

For the binding studies, the [CuL] concentration was kept constant at 15 μM and ctDNA concentration was increased step by step (0-32 μM). For each step, the same amounts of the ctDNA were added to both the [CuL] and the reference solutions [58].

For the competitive displacement experiments, 20 μM solutions of the MB and EB intercalators in the same buffer were prepared and 20 μM of ctDNA solution was added to each solution. Keeping the intercalator and DNA concentrations constant, the [CuL] with varying (0-10 μM) concentrations were mixed and absorption spectra were measured. For the relative viscosities, ctDNA concentration was kept constant at 20 μM and the [CuL] concentration was varied (0-10 μM).

2.4 Theoretical Calculations

2.4.1 The Systems of Interest

In calculations, a double stranded DNA base pairs of 5'-Deoxyguanosine – phosphate- Deoxycytidine-3', $d(GpC)_2$, was used as the intercalation region. All the calculations were carried out in gas phase and water solvent [56].

During the calculations, no restrictions have been applied. All the geometries for the [CuL] ligand, the DNA pairs, and the [CuL]-DNA intercalated complexes were relaxed to their minimum energies without freezing any atom or applying any restrictions. In addition, symmetry constraints were also removed from all the calculations. All the optimizations were confirmed for their minima by frequency calculations.

For the calculations of the free [CuL], the initial structure was taken from our XRD data. For the optimization of the DNA base pairs (without the ligand), we have used two different starting molecules. First, $d(GpC)_2$ slice of the dodecamer B-DNA (PDB id=1BNA) was directly used. Second, we removed the ligand of a known intercalated DNA pairs, in which the base pairs were wide open, and let the DNA pairs relax to the normal distances. Both starting geometries were converged to the same structure.

Similarly, for the calculations the [CuL] intercalated DNA pairs, initial structures of, two starting geometry were considered. First, the X-ray structure of a known structure (with PDB id= 454D), in which a different ligand is intercalated to the $d(GpC)_2$ pairs, was taken and cut to include only the intercalated region. Then, [CuL] was replaced with the ligand, and optimization was carried out. In the second starting geometry, a dummy insertion of the [CuL] into the $d(GpC)_2$, which was extracted from the dodecamer (PDB id=1BNA) without any modification. Both structures were converged to the same intercalated complex.

2.4.2 The Method & Basis Set

Here, we report the interaction of the [CuL] with only the intercalation pocket $d(GpC)_2$ in the QM level ignoring the mechanical part in order to show the possibility of intercalation alone.

Due to the large size of the systems, the calculations can easily be too costly. Thus, the systems should be as small as single base pairs for post Hartree-Fock methods such as additional second order correlation functions (MP2) [59] or computationally more efficient DFT methods. Most DFT

methods failed [59-62] for the inclusion of long distance dispersion forces, hydrogen bonds between the base pairs, and π-π stacking interaction that is responsible for the intercalation [63, 64]. Recent DFT studies such as B3LYP, CAM-B3LYP, M05-2X and M06-2X have been successfully performed to describe the covalency, π-π stacking interaction and hydrogen bonding [3, 38, 45, 47, 65, 66]. Among these, M06-2X [3, 38, 45, 47, 66] and BP86 [65] are widely used for their capabilities of describing hydrogen bonding in Watson-Crick base pairs as well as π-π stacking interactions [67].

Thus, in our calculations we have used M06-2X with Stuttgart/Dresden (SDD) basis set with (quasi relativistic) effective core (10 electrons) potential (ECP) on Cu^{2+} and 6-31G(d) for the rest of the atoms. We have evaluated that increasing the basis set for the non-copper atoms to 6-311++G(d,p) is affecting only in ~1 kJ/mol for the [CuL] complex. And the basis set superposition error (BSSE) was negligible. Thus, we believe this basis set is sufficient for describing the C, H, O, N, and P atoms.

Integral Equation Formalism of a Polarizable Continuum Model (IEF-PCM) was used to include the solvent effects. And default water parameters were used as the PCM water solvent. Routinely, after each optimization process, a frequency calculation was carried out in order to make sure the minimum reached.

3. Results & Discussions

3.1 Experimental and Theoretical Study of [CuL]

In order to understand the nature of the intercalation, we first analyzed the photophysical behavior of the [CuL] complex. The bimorphous crystal structure of H_2L ligand shows that one of the aromatic salicyl rings is twisted by 46°, distorting the Cs symmetrical structure (Table 1). The twist on the other aromatic salicyl ring is very little (2°) due to the intra-ligand hydrogen bonding to the pyridine N atom. Upon addition of the Cu(II) ion, the salicyl rings are restricted to stay aligned to the pyridine ring. The highly twisted ring on H_2L is rotated by ~50° to become 4° in [CuL]. The untwisted ring is not affected by Cu^{2+}. The calculations in PCM water solvent are in excellent agreement in estimating structural change upon complexation of the H_2L ligand. According to the calculations, the H_2L ligand holds the twisted ring by 42° and [CuL] structure adopts a Cs symmetrical structure with both salicyl rings 0°. We believe the larger size of the planar group in the [CuL] structure can activate it for the intercalation since the size of the planar groups is critical for intercalation.

Table 1. Selected bond distances and dihedral angles for the H_2L ligand and [CuL] complex. Only the heavy atoms around the Cu(II) are given. The dihedral angles belong to the ones between pyridine ring and salicyl rings (See Figure 1). All the calculations are in water PCM environment

Molecule	ϕ (°)	ϕ' (°)	Cu-O1 (Å)	Cu-O2 (Å)	Cu-N2 (Å)	Cu-N3 (Å)
Experimental H_2L	-46	-2				
Calculated H_2L	-42	-3				
Experimental [CuL]	4	-2	1.89	1.88	1.93	1.94
Calculated [CuL]	0	0	1.92	1.91	1.99	2.00

In the [CuL] complex, experimental bond lengths of Cu—O and Cu—N are 1.89-1.88 Å and 1.93-1.94 Å, respectively (Table 1). The calculations predict similar bond distances. These strong bonds are typical for the metal ions with empty 4s orbitals and partially occupied 3d orbitals. The effect of size and electronic configuration of metal ions such as $Mn^{+}(3d^{5}4s^{1})$ [68], $Fe^{+}(3d^{6}4s^{1}$ or $3d^{7}4s^{0})$ [69], Co^{+} $(3d^{8}4s^{0})$ [70, 71], $Ni^{+}(3d^{9}4s^{0})$ [70, 72], $Cu^{+}(3d^{10}4s^{0})$ [73], and $Ag^{+}(4d^{10}5s^{0})$ [73] on the bond strength and coordination is well documented in literature. Since the size of 4s orbital is larger than that of 3d orbitals, the repulsion between the metal and ligand is smaller in the systems in which 4s orbitals are empty, so the ligand can come closer to the metal ion. In addition, the 3d orbitals are directional while 4s orbitals are spherical. This means the electrons on 3d orbitals can be localized in order to minimize the repulsion. Thus, the ligand can come closer to the metal ion, resulting with stronger M-L bond [69-72].

Demir et al. reported the experimental UV-VIS spectra of the H_2L ligand and [CuL] complex in methanol solutions [51]. Our experimental findings for the [CuL] in the Tris buffer (with 5% DMF) are very similar. The Figure 2 shows the absorption spectrum of the [CuL] in the buffered aqueous solution. There is an intense absorption band at 262 nm (ε=15930 $L.mol^{-1}.cm^{-1}$), a broad and intense band at 322 nm (ε=21530 $L.mol^{-1}.cm^{-1}$) with two shoulders at 293 nm and 342 nm, and another broad band starting at 364 nm and peaking at 408 nm (ε=21600 $L.mol^{-1}.cm^{-1}$). The overall pattern of the spectrum is very similar to those of Fe(III), Zn(II), Ni(II) and Cu(II) –salen and salphen complexes, all of which have been reported to adopt a square planar coordination around the metal center [3, 67, 74]. For such systems, it was reported that the low lying

band is due to π–π* transition while the higher wavelength bands are due to metal and solvent perturbed intra-ligand electronic transition [3, 74, 75].

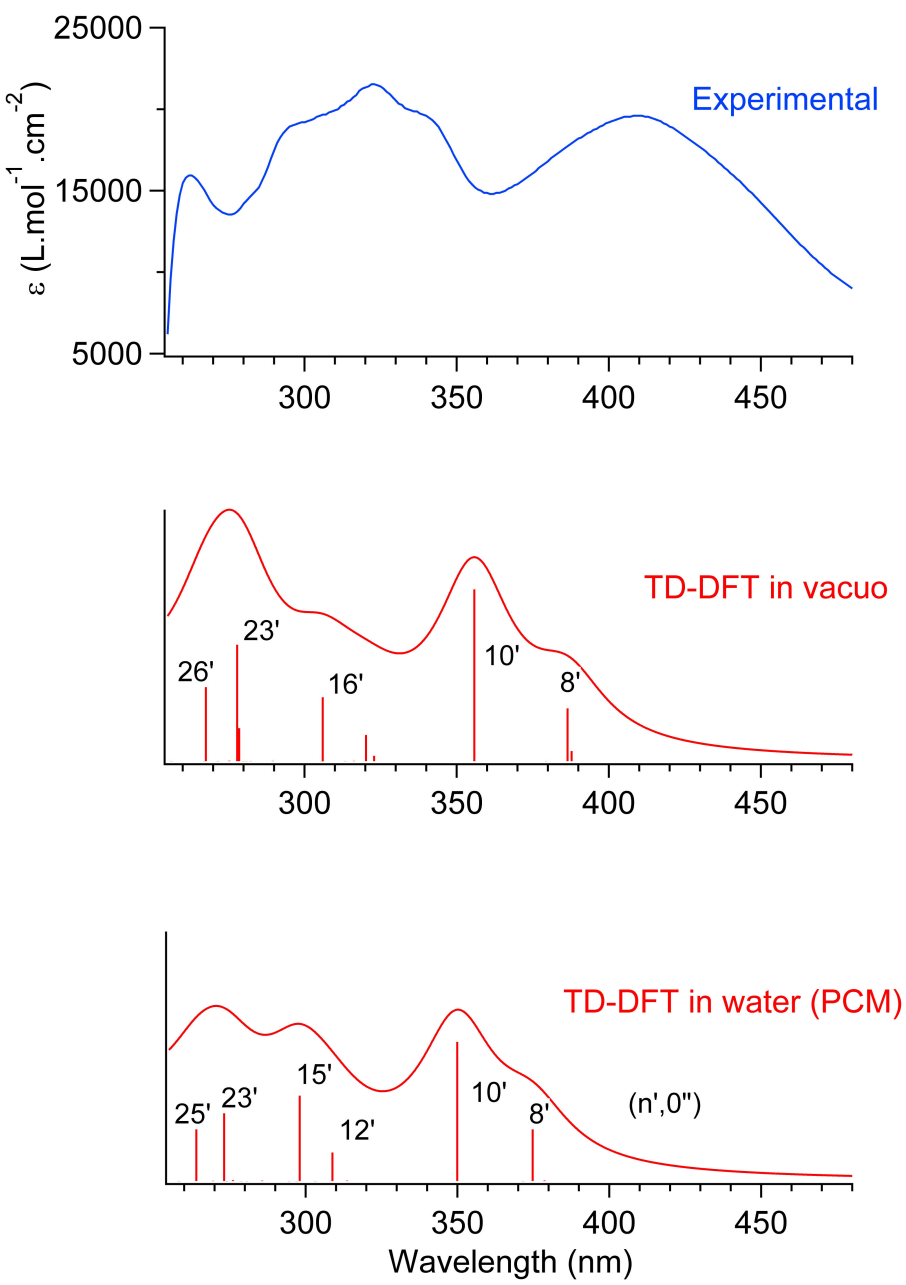

Figure 2. The electronic absorption spectra of [CuL] (a) experimental (top) and theoretical UV-Vis spectra of [CuL] (b) in vacuo (middle), and (c) in PCM water environment (bottom). Vertical lines and numbering show the transition from the ground state to the regarding electronic excited state.

.

The ground and excited state calculations (Figure S2) show that [CuL] complex has an additional band in the high wavelength region suggesting ligand-to-metal charge transfer (LMCT) at 375 nm besides the intra-ligand electronic transitions at 350 nm, which is also observed for the H_2L ligand at 331 nm. The Cu^{2+} ion causes the planarization of the system increasing the electron fluency and reducing the band gap between the charge transfer orbitals, thus, resulting with red shift on the transition.

In order to understand the solvent effect, we compared calculations in solution environment. Figure 2 shows comparison of the experimental UV-VIS spectrum of [CuL] to the calculated ones in gas phase and water. As it can be seen, the bands of calculated spectra are consistently blue-shifted from the experiment, and the shift is smaller in the low wavelength region. Surprisingly, this blue-shift gets even larger upon inclusion of the water solvent effect. However, in terms of relative transition intensities, the solvent effect makes the spectra better match to the experiment.

To investigate the insights for the transitions with high oscillator strengths, we also performed Natural Transition Orbital (NTO) analysis [76]. This method is a compact orbital representation for electronic transition density matrix and gives a maximal correspondence between the excited and empty orbital pairs (particle/hole NTO pairs) [76]. Figure 3 shows the most dominant NTO pairs and their contributions to related transitions. It shows that the bands at 375 nm and 350 nm are mostly due to intra-ligand transitions, and metal involvement in the transitions is very small. However, it carries some charge transfer and planarization plays an important role on that. The

transitions that are just below 300 nm are also involved some charge transfer character but these are barely perturbed by the metal ion (Figure S2). On the other hand, the lowest wavelength transition is strongly affected by the metal. For the allowed transitions, vertical excitation energies in the PCM water solvent, the molecular orbital contributions and corresponding NTOs are listed in Table 2. Highly mixed molecular orbitals, especially at higher energy region, is much more explained by the NTO analysis. However, we should note that the Cu^{2+} is open-shell ($3d^9 4s^0$) and the percent contributions are not normalized. Thus only alpha molecular orbitals are listed here (for the beta orbitals, see Table S2).

The transitions due to DNA sandwiched π-stacking can be observed at 200-300 nm region, depending on the buffer environment, which overlaps with the low lying transitions of the [CuL] complex. However, the DNA shows almost no absorption above 300 nm.

.

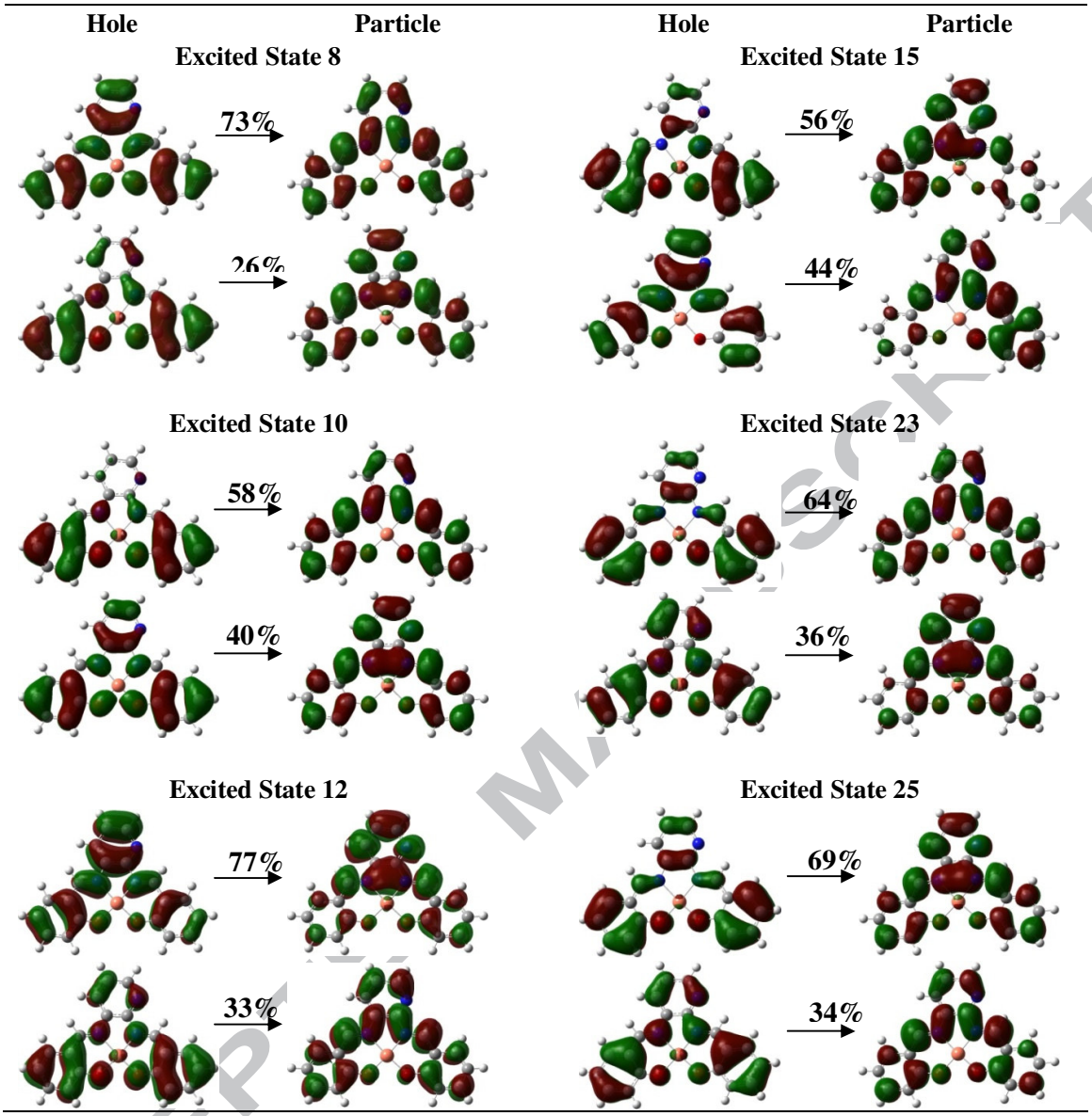

Figure 3. Most dominant NTO pairs belonging the transitions with oscillator strength, f>0.1, for [CuL] in PCM water solvent. The contributions of alpha spin NTOs for each transition are also shown. Corresponding oscillator strengths and amplitudes of SCF orbitals are presented in Table 2 (For beta spin NTOs, see Table S2).

Table 2. Transition energies, intensities and orbitals from vertical excitations. Calculations are in water (PCM) environment. For the orbital descriptions only alpha orbitals are given without normalization. For the corresponding beta contributions, see Table S2

Excited State	ΔE (eV)	*f*	SCF Orbitals (SCFO) Description	NTO Description
8	3.31	0.2049	$-0.33997(\psi_{H-1}\rightarrow\psi'_{L+1})$ $+0.59649(\psi_{H}\rightarrow\psi'_{L})$	$0.73(\phi_{H}\rightarrow\phi'_{L})$ $+0.26(\phi_{H-1}\rightarrow\phi'_{L+1})$
10	3.54	0.5462	$0.53284(\psi_{H-1}\rightarrow\psi'_{L})$ $-0.43925(\psi_{H}\rightarrow\psi'_{L+1})$	$0.58(\phi_{H}\rightarrow\phi'_{L})$ $+0.40(\phi_{H-1}\rightarrow\phi'_{L+1})$
12	4.01	0.1124	$0.11533(\psi_{H-5}\rightarrow\psi'_{L+1})$ $+0.27160(\psi_{H-2}\rightarrow\psi'_{L+1})$ $+0.40256(\psi_{H-1}\rightarrow\psi'_{L})$ $+0.53439(\psi_{H}\rightarrow\psi'_{L+1})$	$0.77(\phi_{H}\rightarrow\phi'_{L})$ $+0.33(\phi_{H-1}\rightarrow\phi'_{L+1})$
15	4.16	0.3349	$0.34583(\psi_{H-2}\rightarrow\psi'_{L})$ $+0.51581(\psi_{H-1}\rightarrow\psi'_{L+1})$ $+0.32441(\psi_{H}\rightarrow\psi'_{L})$	$0.56(\phi_{H}\rightarrow\phi'_{L})$ $+0.44(\phi_{H-1}\rightarrow\phi'_{L+1})$
23	4.54	0.3031	$-0.26706(\psi_{H-3}\rightarrow\psi'_{L+1})$ $+0.51958(\psi_{H-2}\rightarrow\psi'_{L})$ $-0.30336(\psi_{H-1}\rightarrow\psi'_{L+1})$ $-0.22812(\psi_{H}\rightarrow\psi'_{L})$	$0.64(\phi_{H}\rightarrow\phi'_{L})$ $+0.36(\phi_{H-1}\rightarrow\phi'_{L+1})$
25	4.70	0.2256	$-0.33435(\psi_{H-3}\rightarrow\psi'_{L})$ $+0.55642(\psi_{H-2}\rightarrow\psi'_{L+1})$ $-0.21928(\psi_{H-1}\rightarrow\psi'_{L})$ $-0.19027(\psi_{H}\rightarrow\psi'_{L+1})$ $+0.11084(\psi_{H}\rightarrow\psi'_{L+3})$	$0.69(\phi_{H}\rightarrow\phi'_{L})$ $+0.34(\phi_{H-1}\rightarrow\phi'_{L+1})$
H:HOMO; L:LUMO; ψ: Occupied SCFO; ψ': Virtual SCFO; ϕ: Occupied NTO; ϕ':Virtual NTO				

3.2 DNA Intercalation

The [CuL] complex synthesized, characterized and analyzed in the first part is a good candidate for being a DNA intercalator. Therefore, we investigated its intercalative behavior both experimentally and theoretically.

3.2.1 DNA Titration by [CuL]

Previous studies have shown that when the ligand-DNA interaction is intercalative, the absorption bands of the ligand shift to higher wavelength (red-shift) and the relative intensities drop drastically (hypochromism) [45, 75]. The absorption spectrum of the [CuL] is perturbed by the addition of ctDNA at increasing concentrations (Figure 4). The spectra show that the absorption band at 323 nm is red shifted by 1 nm and shows 60% of hypochromism. Similarly, the band at 408 nm is red shifted by 4 nm and shows a 50% of drop in the intensity. This clearly shows the intercalative interaction between DNA and [CuL] complex. However, the band at 262 nm is red shifted and the intensity drops upon addition of the DNA up to reaching the equivalent DNA concentration ([DNA]/[CuL]=1). After that it behaves differently and 3 nm blue-shifted band at 259 nm raises with further additions of DNA. This behavior is explainable and actually confirms the intercalative interaction. The idea behind that is as follows. In the 250-260 nm region both the free DNA and free [CuL] absorbs in the $\pi \rightarrow \pi^*$ transition. However, when the intercalation occurs, the π–π stacking interaction between the aromatic rings of the [CuL] and DNA base pairs, which results with less $\pi \rightarrow \pi^*$ transitions in the [CuL]-DNA complex. Initially, the absorption is due to completely free [CuL] since no DNA is available. With the addition of DNA

up to the stoichiometric ratio, the [CuL] concentration is diminished by the formation of the intercalated complex which has very little absorption due to the stacking interaction. Thus, for these concentrations the absorption decreased. On the other hand, when there is excess amount of DNA, the absorption is mostly due to DNA base pairs and it increases depending on the free DNA in the media. This behavior is also observed for Cu(II) complexes of similar salphen type ligands [74].

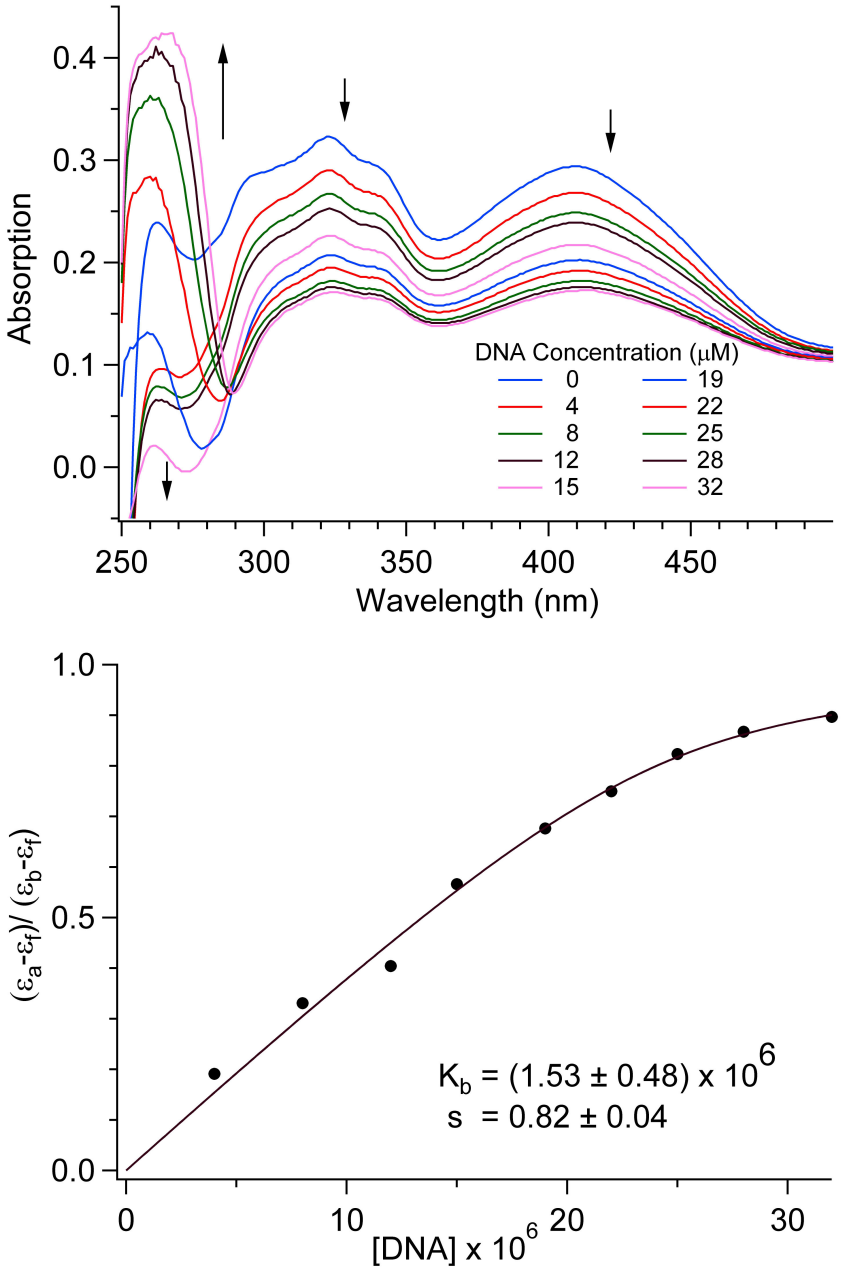

Figure 4. a) Absorption spectra (top) for the titration of [CuL] by increasing concentrations of ctDNA in the Tris/HCl buffer pH=7.2 and I=0.1 M (NaCl). The vertical arrows show the trend in the absorption intensity with the increasing DNA concentration. b) The nonlinear-fit (bottom) using the eq (4) of [DNA] at 408 nm.

The typical red shift value for strong interaction is ~15-25 nm [45, 74]. Our experimental red-shifts (1-4 nm) are suggesting somewhat weak interaction.

From the absorption titrations, the interaction strength can be quantified by finding the binding constant of the [CuL] to DNA. The quadratic formula to find the binding constant derived by Bard and co-workers [77] can be utilized for the titration. Considering the binding of the ligand, L, to a DNA binding site of, D, which is composed of s base pairs of total number of nucleotides, N, forming an intercalated species, D-L, a non-cooperative interaction, in which there is only one type of binding site and the ligand does not bind sequence selectively, can be represented as [77]:

$$L + D = D - L \quad (1)$$

The binding constant is given with;

$$K_b = \frac{C_b}{C_f C_d} \quad (2)$$

Where, C_b, C_f, and C_d are equilibrium concentrations of bound ligand, free ligand, and free binding site, respectively.

The total ligand concentration, C_t is: $C_t = C_b + C_f$

The total DNA concentration in monomer unit: $\frac{[DNA_{mono}]}{2.s} = C_b + C_d$

Where, s is the number of the base pairs that are interacting with ligand. Including these terms in the equation (2),

$$K_b C_b^2 - (1 + K_b C_t + \frac{K_b[DNA_{mono}]}{2s})C_b + \frac{K_b C_t[DNA_{mono}]}{2s} = 0 \qquad (3)$$

The eq. (3) can be readily solved for C_b using the quadratic formula. Assuming the apparent Absorption (A_a) to be sum of free (A_f) and bound absorptions (A_b),

$$A_a = A_f + A_b$$

$$\varepsilon_a C_t = \varepsilon_f C_f + \varepsilon_b C_b = \varepsilon_f (C_t - C_b) + \varepsilon_b C_b$$

Thus C_b can be represented as [78];

$$C_b = C_t \frac{\varepsilon_a - \varepsilon_f}{\varepsilon_b - \varepsilon_f}$$

Thus, solution to the equation becomes;

$$\frac{\varepsilon_a - \varepsilon_f}{\varepsilon_b - \varepsilon_f} = \frac{b - \sqrt{b^2 - \frac{2K_b^2 C_t[DNA_{mono}]}{s}}}{2K_b C_t} \qquad (4)$$

Where,
$$b = 1 + K_b C_t + \frac{K_b[DNA_{mono}]}{2s}$$

In the eq. (4) [77], the ε_f, ε_b, and ε_a are the molar extinction coefficients of a) free [CuL] ligand in the absence of DNA b) bound [CuL]-DNA in stoichiometric ratio c) apparent mixture of [CuL], DNA and [CuL]/DNA when both [CuL]-DNA complex and either one of the [CuL] or DNA is freely, respectively, available. The ε_f is a constant value and can be determined from the calibration curve of the free [CuL] complex, using the Beer-Lambert law. The ε_b constant value can be determined from the plateau of the titration curve where no more change in the absorption is observed. The ε_a is a varying value and is determined from the ratio of the measured absorbance to the constant

[CuL] initial concentration value. The experimental titration curve of $\frac{\varepsilon_a-\varepsilon_f}{\varepsilon_b-\varepsilon_f}$ vs. $[DNA_{mono}]$ is shown in Figure 4. The K_b and s coefficients can be obtained by nonlinear least-squares fitting of the experimental data using the eq. (3).

The band at 408 nm in Figure 4 includes no contribution from the DNA absorption. For this reason, the experimental binding constant K_b and binding site size s were determined from this band as (1.53 ± 0.48) x 10^6 M^{-1} and (0.82 ± 0.04). This K_b value confirms that the interaction is strong. The proximity of the s value to 1 confirms that the binding is intercalative in which 1 ligand per base pair interacts. This binding constant is similar to those of EB and MB (For EB-ctDNA, K_b=1.7 x 10^5 M^{-1} [79] (1.4 x 10^6 M^{-1} on ref. [80]) and for MB-ctDNA, K_b=2.32 x 10^5 M^{-1} [81] (1.13 x 10^6 M^{-1} on ref. [82]). Both the EB and MB have been studied numerously as their excellent fluorometric behavior upon binding to the DNA. Thus, these two compounds are widely used as competitive probes.

3.2.2 MB and EB Competitive Displacement Assays

We also carried out further experiments in order to ensure that the [CuL] interacts with the ctDNA more strongly than the EB and MB. The idea is that the absorption spectra of EB and MB are red shifted by DNA intercalation, and if the ligand exchange reactions occur between the ligands of [CuL] and of EB and MB, the free EB and MB concentrations will increase recovering the shift in the spectra. The Figure 5 (bottom) shows change in the absorption spectra of the intercalated EB-DNA (20 μM, 1:1 solution) by addition of [CuL]. As can be seen from the spectra, the free EB (solid blue line) maximum

absorption band at 480 nm shifts to 493 nm and the intensity is reduced by 35% due to the DNA intercalation (solid black line). However, with the addition of increasing concentrations of the [CuL], the intensity (dashed red lines) re-increases and it blue-shifts, almost fully recovering to the free EB absorption spectrum. This confirms that the [CuL] strongly binds to the DNA in the same region by kicking the EB. The Figure 5 (top) shows the same procedure applied to the MB. The free MB ligand (solid blue line) has an absorption maximum at 662 nm, which shifts to 668 nm when intercalated to the ctDNA (solid black line). When MB-DNA intercalated complex is treated with the increasing concentrations of [CuL] ligand, the intensity and red-shift are recovered by ~35% (dashed red lines).

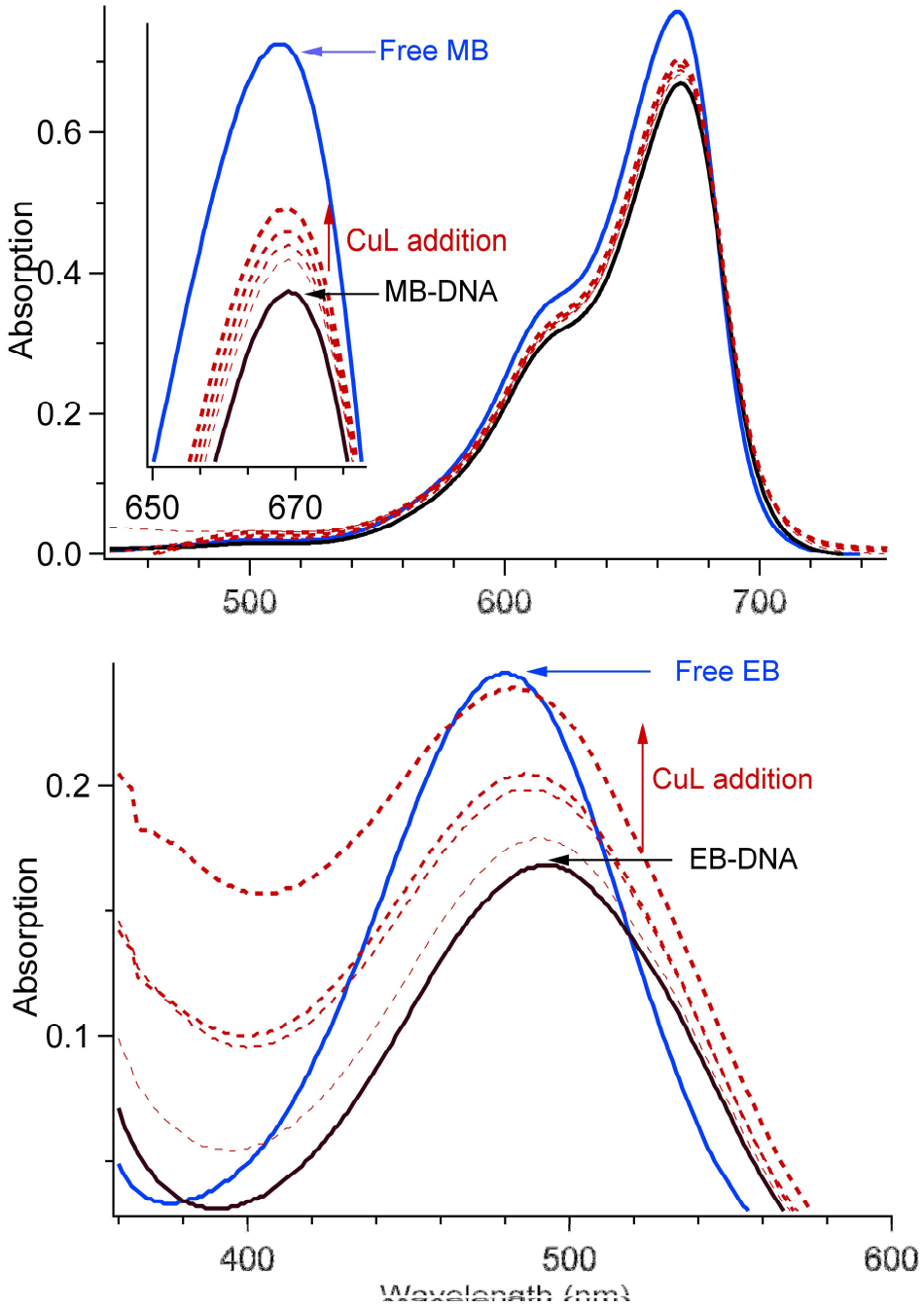

Figure 5. Absorption spectra for competitive displacement assays of [CuL] with (a) MB (top) and (b) EB (bottom). The solid black lines represent absorption of MB or EB fully intercalated in ctDNA with the absent of [CuL]. By addition of the [CuL] (dashed lines, increasing thickness according to the concentration), the absorption approaches the free MB/EB spectra.

3.2.3 Viscosity

Lerman [83] showed that viscosity of rod-like calf thymus (double stranded) DNA increases with the increase of the intercalating ligand amounts. The increase in viscosity happens due to an increase of the DNA duplex length (L) upon intercalation [84, 85]. The viscosity of DNA can be expressed as flow times of the buffer (t_0) and the DNA (t) solutions.

$$\eta = (t - t_0)/t_0$$

Since the viscosity is proportional to L^3, relative viscosity values of the DNA the presence (η) and in the absence ($\eta°$) of ligand is given as $(\eta/\eta°)^{1/3}$ versus the binding ratio[86], $r_{total} = \frac{[Ligand]}{[DNA]}$.

The Figure 6 shows the relative viscosity increase by addition of [CuL] ligand to DNA containing buffer, which confirms the intercalation of the DNA by the [CuL].

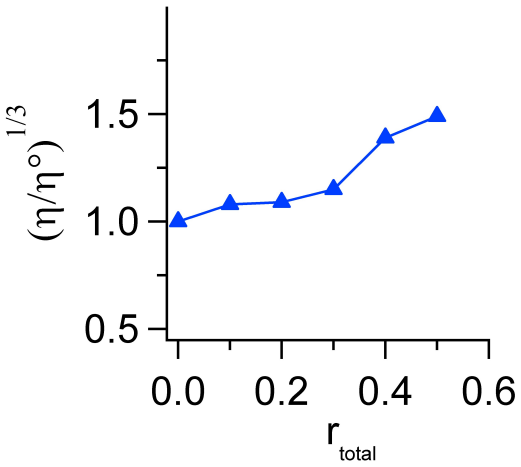

Figure 6. Plot of relative viscosity $(\eta/\eta°)^{1/3}$ of ctDNA versus r_{total} at 25 °C in the Tris buffer with pH=7.2 and I=0.1 M (NaCl). Each measurement was made with average flow rates of 3 repetitive flow times.

3.3 Comparison of calculations to experiments

The [CuL] complex can interact with the DNA in an intercalative way or minor/major groove electrostatic interaction. As the experimental studies suggested, here we report only intercalative interaction on $d(GpC)_2$ pocket. Since the effects of sugar and charged phosphate groups are important [45, 47] we have optimized the structures including these moieties. The Figure 7 shows the optimized structures of both intercalated [CuL]-DNA complex and free $d(GpC)_2$ in water (PCM).The changes on the geometry of the DNA upon interacting with the [CuL] are summarized in Table 3.

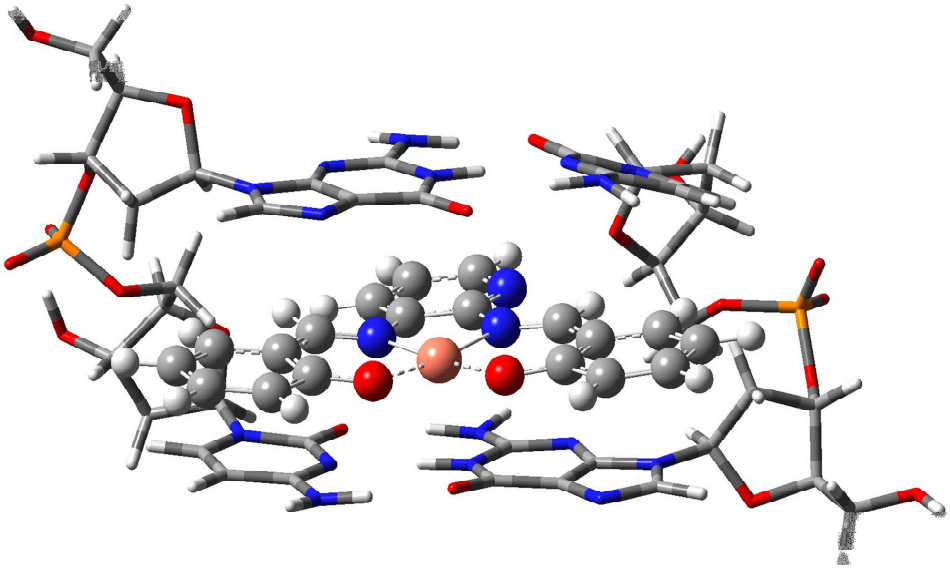

Figure 7. Optimized molecular structure of [CuL] intercalated in $d(GpC)_2$. Calculations were carried out using M06-2X level with SDD-ECPs for the Cu^{2+} and 6-31G(d) for the rest of the atoms. Two different starting geometries, inserting at the intercalation pocket of the free B-DNA (pdb id: 1BNA) and replacing the [CuL] with a known intercalated ligand (pdb id:454D), were converged to the same structure.

Table 3. Some selected bond lengths and angles of X-ray crystallography and geometry optimization calculations. Labels of the first column are referring the centroids and planes (described in the text).

	Experimental	Calculations		
	Base pairs only (1BNA)	Base pairs only (1BNA)	Base pairs only (454D)	Intercalated [CuL]-DNA (454D)
C1-G1	5.4	5.6	5.5	5.6
C2-G2	5.6	5.7	5.5	5.6
G1-C2	3.5	3.4	3.8	6.6
C1-G2	4.3	4.4	4.1	6.2
<PC1-PG2	26.3	26.3	6.1	20.6
<PG1-PC2	4.7	4.8	3.7	3.7
<PC1-PG1	22.3	22.4	12.2	18.3
<PC2-PG2	12.9	12.6	7.8	5.1

We describe the distances and angles by creating a centroid on each six membered ring of DNA bases and a plane for each six membered ring, covering all the atoms on the ring. Upon binding, distance of the inter-base pairs (base pair step) rises. The G1-C2 goes from 3.4 Å (in 454D, same value is 3.8 Å in 1BNA) to 6.6 Å and C1-G2 distance of 4.4 Å (in 454D, same value is 4.1 Å in 1BNA) increases to 6.2 Å (Table 3). Such a nearly doubling of the distances is typical for an intercalation. The intra-base pair hydrogen bonds are maintained in the intercalated complexes, thus the distances of C1-G1 and C2-G2 in [CuL]-DNA are almost the same as free DNA, 5.6 ± 0.1 Å. The angles of the planes, on the other hand, show quite differences upon the intercalation. The PG2 plane appears to be the most flexible and rotates, which affects mostly <PC1-PG2, changing from 26.3° (on 454D) to 20.6°, and <PC2-PG2, from 12.6° (on 454D) to 5.1°. Although, this change can be attributed to opening of the double strand, we know that the angles don't have great impact on the energy of the molecule. Therefore, having great change on the angles may not mean great change in the stability of the molecule. In addition, the

correct plane angles in free DNA molecules are already quite different between the 454D and 1BNA structures.

Calculated binding energies are given in Table 4 for both gas and water solution phases. The values are in qualitatively agreement with the experimental value. The binding energy in the gas phase is larger. This shows that water solvent destabilizes the DNA-[CuL] complex.

Table 4. The calculated binding energies of [CuL] in the DNA base pairs. The values are bottom of the well values and do not include zero point energies and thermal energies.

	Gas Phase		Water (PCM) Solvent	
	SCF Energy (Hartree)	Binding Energy (kJ/mol)	SCF Energy (Hartree)	Binding Energy (kJ/mol)
[CuL] Ligand	-1243.5827	-	-1243.60039	-
DNA Base Pair, $d(GpC)_2$	-4539.1101	-	-4539.34549	-
[CuL]-DNA Complex	-5782.7218	-76.2	-5782.953215	-19.3

Figure 8 compares the experimental spectra of isolated [CuL] and [CuL]-ctDNA complex (top) along with calculated spectra of [CuL] and [CuL]-$d(GpC)_2$ intercalated systems. The change in the experimental spectrum upon binding to the ctDNA is totally reproduced by the calculations. The overall intensity is reduced by intercalation in both experimental and calculated spectra. All of the three bands in the spectra are affected by intercalation. In addition, perfectly agreeing with the experiment, the intercalation is calculated to have a 9 nm of red shift in the lowest energy band, which is observed as 4 nm.

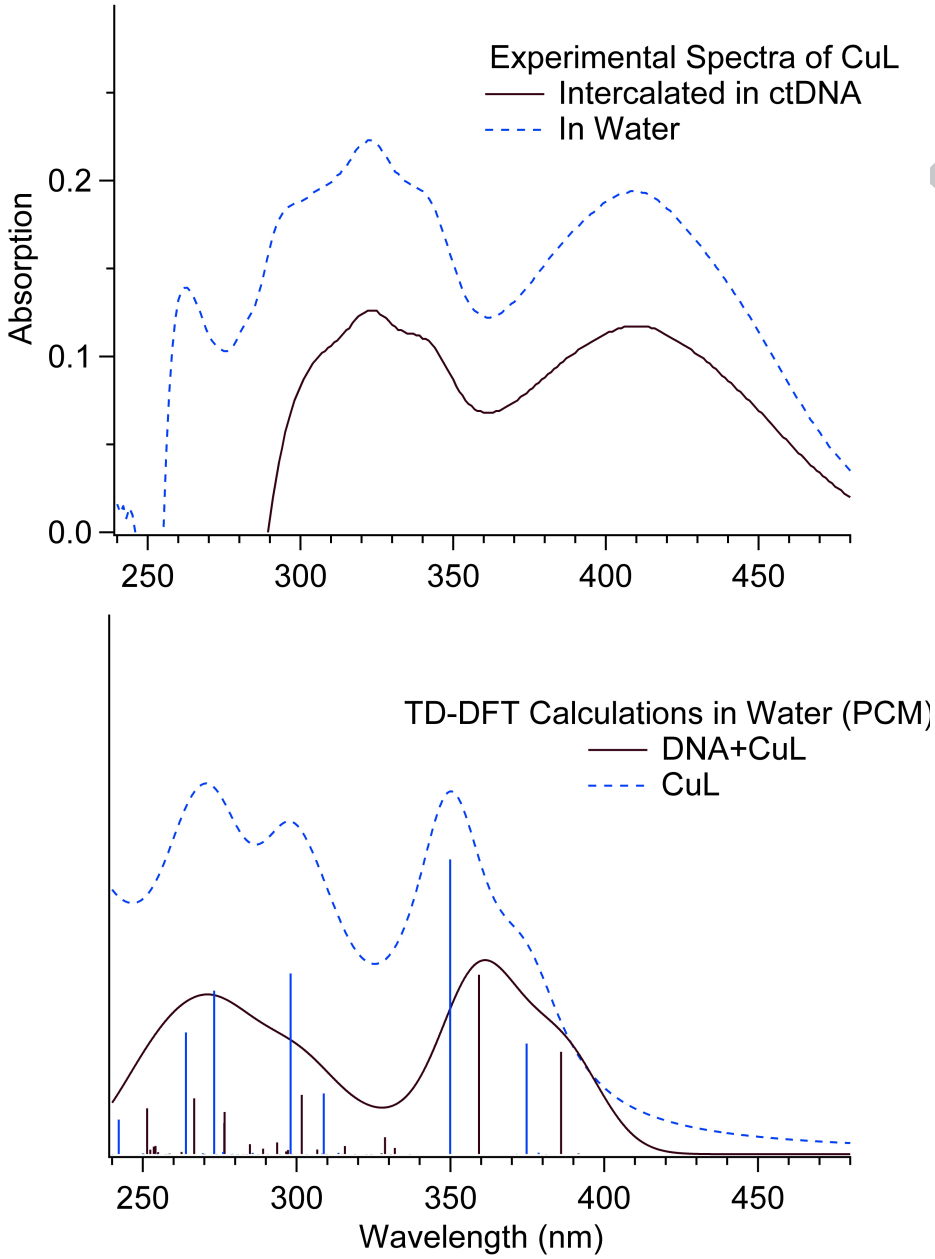

Figure 8. Comparison of (a) the experimental absorption spectra (top) with (b) simulation of calculated vertical electronic transitions (bottom) of [CuL] in water (dashed blue) and in ctDNA (solid black). Experimental spectra (of both in water and ctDNA) are measured in the Tris buffer with pH=7.2 and I=0.1 M (NaCl). The calculations are in PCM water for both free [CuL] and intercalated in $d(GpC)_2$ and use M06-2X level with SDD-ECPs for the Cu^{2+} and 6-31G(d) for the rest of the atoms. Lorentzian type function with 30 nm line-width is used for the simulations. Blue and black vertical lines show the electronic transition wavenumbers.

4. Conclusions

Here, we demonstrate the possibility of finding the DNA binding drugs by showing the interaction of a new salphen ligand with ctDNA. The Cu^{2+} ion modifies the Schiff base (H_2L) by aligning the aromatic rings (planarization), thus forms [CuL], an active DNA intercalator. The intercalation process was sensitively interpreted by the characteristic experimental and calculated absorption spectra of the [CuL]. The calculated spectra of [CuL] intercalated in the DNA base pairs reproduced correctly the red shift and intensity drop on the spectrum. Qualitatively, experimental binding energy was in agreement with calculations.

Appendix A: Supplementary Data

CCDC 1418016 and 1418030 contain the supplementary crystallographic data for H_2L and [CuL], respectively. These data can be obtained free of charge via http://www.ccdc.cam.ac.uk/conts/retrieving.html, or from the Cambridge Crystallographic Data Centre, 12 Union Road, Cambridge CB2 1EZ, UK; fax: (+44) 1223-336-033; or email: deposit@ccdc.cam.ac.uk.

Appendix B: Supplementary Data

Acknowledgements

A.K and H.Y gratefully acknowledge Ricardo B. Metz from the University of Massachusetts; Hatice Can and Ali Turkan from Gebze Technical University; Serkan Demir from Giresun University and TUBITAK for their

valuable advice and allowing to use their computer clusters and software packages for calculations.

References

[1] S.U. Rehman, Z. Yaseen, M.A. Husain, T. Sarwar, H.M. Ishqi, M. Tabish, PLoS ONE, vol. 9, Public Library of Science, 2014, pp. e93913.

[2] G. Barone, A. Terenzi, A. Lauria, A.M. Almerico, J.M. Leal, N. Busto, B. García, Coordination Chemistry Reviews, vol. 257, 2013, pp. 2848-2862.

[3] A. Lauria, R. Bonsignore, A. Terenzi, A. Spinello, F. Giannici, A. Longo, A.M. Almerico, G. Barone, Dalton Transactions, vol. 43, The Royal Society of Chemistry, 2014, pp. 6108-6119.

[4] M.J. Hannon, Chemical Society Reviews, vol. 36, The Royal Society of Chemistry, 2007, pp. 280-295.

[5] E.N. Jacobsen, in: E.W.A.G.A.S. Wilkinson (Ed.), Comprehensive Organometallic Chemistry II, Elsevier, Oxford, 1995, pp. 1097-1135.

[6] T.M. Ovitt, G.W. Coates, Journal of the American Chemical Society, vol. 121, American Chemical Society, 1999, pp. 4072-4073.

[7] D.A. Atwood, M.J. Harvey, Chemical Reviews, vol. 101, American Chemical Society, 2001, pp. 37-52.

[8] C.T. Cohen, T. Chu, G.W. Coates, Journal of the American Chemical Society, vol. 127, American Chemical Society, 2005, pp. 10869-10878.

[9] L. Canali, D. C. Sherrington, Chemical Society Reviews, vol. 28, The Royal Society of Chemistry, 1999, pp. 85-93.

[10] R.G. Konsler, J. Karl, E.N. Jacobsen, Journal of the American Chemical Society, vol. 120, American Chemical Society, 1998, pp. 10780-10781.

[11] A.W. Kleij, M. Kuil, D.M. Tooke, M. Lutz, A.L. Spek, J.N.H. Reek, Chemistry – A European Journal, vol. 11, WILEY-VCH Verlag, 2005, pp. 4743-4750.

[12] A.W. Kleij, M. Kuil, M. Lutz, D.M. Tooke, A.L. Spek, P.C.J. Kamer, P.W.N.M. van Leeuwen, J.N.H. Reek, Inorganica Chimica Acta, vol. 359, 2006, pp. 1807-1814.

[13] Pascal G. Lacroix, European Journal of Inorganic Chemistry, vol. 2001, WILEY-VCH Verlag GmbH, 2001, pp. 339-348.

[14] R. Brissos, D. Ramos, J.C. Lima, F.Y. Mihan, M. Borras, J. de Lapuente, A.D. Cort, L. Rodriguez, New Journal of Chemistry, vol. 37, The Royal Society of Chemistry, 2013, pp. 1046-1055.

[15] S.I. Pascu, P.A. Waghorn, T.D. Conry, B. Lin, H.M. Betts, J.R. Dilworth, R.B. Sim, G.C. Churchill, F.I. Aigbirhio, J.E. Warren, Dalton Transactions, The Royal Society of Chemistry, 2008, pp. 2107-2110.

[16] G. Consiglio, S. Failla, P. Finocchiaro, I.P. Oliveri, S.D. Bella, Dalton Transactions, vol. 41, The Royal Society of Chemistry, 2012, pp. 387-395.

[17] A.L. Singer, D.A. Atwood, Inorganica Chimica Acta, vol. 277, 1998, pp. 157-162.

[18] Y. Gao, J. Wu, Y. Li, P. Sun, H. Zhou, J. Yang, S. Zhang, B. Jin, Y. Tian, Journal of the American Chemical Society, vol. 131, American Chemical Society, 2009, pp. 5208-5213.

[19] M. Cano, L. Rodríguez, J.C. Lima, F. Pina, A. Dalla Cort, C. Pasquini, L. Schiaffino, Inorganic Chemistry, vol. 48, American Chemical Society, 2009, pp. 6229-6235.

[20] I.P. Oliveri, S. Di Bella, The Journal of Physical Chemistry A, vol. 115, American Chemical Society, 2011, pp. 14325-14330.

[21] E.C. Escudero-Adán, J. Benet-Buchholz, A.W. Kleij, Inorganic Chemistry, vol. 47, American Chemical Society, 2008, pp. 4256-4263.

[22] S. Khatua, S.H. Choi, J. Lee, K. Kim, Y. Do, D.G. Churchill, Inorganic Chemistry, vol. 48, American Chemical Society, 2009, pp. 2993-2999.

[23] Y. Hamada, T. Sano, M. Fujita, T. Fujii, Y. Nishio, K. Shibata, Jpn. J. Appl. Phys. 2, vol. 32, 1993, pp. L511.

[24] T. Sano, Y. Nishio, Y. Hamada, H. Takahashi, T. Usuki, K. Shibata, Journal of Materials Chemistry, vol. 10, The Royal Society of Chemistry, 2000, pp. 157-161.

[25] M.E. Germain, T.R. Vargo, P.G. Khalifah, M.J. Knapp, Inorganic Chemistry, vol. 46, American Chemical Society, 2007, pp. 4422-4429.

[26] A. Rajendran, C.J. Magesh, P.T. Perumal, Biochimica et Biophysica Acta (BBA) - General Subjects, vol. 1780, 2008, pp. 282-288.

[27] A. Arola-Arnal, J. Benet-Buchholz, S. Neidle, R. Vilar, Inorg. Chem., vol. 47, 2008, pp. 11910.

[28] B. Peng, W.H. Zhou, L. Yan, H.W. Liu, L. Zhu, Transition Metal Chemistry, vol. 34, 2009, pp. 231-237.

[29] G.D. Liu, J.P. Liao, S.S. Huang, G.L. Shen, R.Q. Yu, Analytical Sciences, vol. 17, 2001, pp. 1031-1036.

[30] G.D. Liu, X. Yang, Z.P. Chen, G.L. Shen, R.Q. Yu, Analytical Sciences, vol. 16, 2000, pp. 1255-1259.

[31] D.J. Gravert, J.H. Griffin, Inorganic Chemistry, vol. 35, 1996, pp. 4837-4847.

[32] K.I. Ansari, J.D. Grant, G.A. Woldemariam, S. Kasiri, S.S. Mandal, Organic and Biomolecular Chemistry, vol. 7, 2009, pp. 926-932.

[33] G.A. Woldemariam, S.S. Mandal, Journal of Inorganic Biochemistry, vol. 102, 2008, pp. 740-747.

[34] S. Bhattacharya, S.S. Mandal, Journal of the Chemical Society, Chemical Communications, 1995, pp. 2489-2490.

[35] S. Routier, J.L. Bernier, M.J. Waring, P. Colson, C. Houssier, C. Bailly, Journal of Organic Chemistry, vol. 61, 1996, pp. 2326-2331.

[36] K. Sato, M. Chikira, Y. Fujii, A. Komatsu, Journal of the Chemical Society - Series Chemical Communications, 1994, pp. 625-626.

[37] G. Barone, A. Ruggirello, A. Silvestri, A. Terenzi, V.T. Liveri, Journal of Inorganic Biochemistry, vol. 104, 2010, pp. 765-773.

[38] A. Spinello, A. Terenzi, G. Barone, Journal of Inorganic Biochemistry, vol. 124, 2013, pp. 63-69.

[39] A. Pérez, F.J. Luque, M. Orozco, Accounts of Chemical Research, vol. 45, American Chemical Society, 2012, pp. 196-205.

[40] C.A. Laughton, S.A. Harris, WIREs Comput. Mol. Sci., vol. 1, 2011, pp. 590.

[41] S. Khalid, P.J. Bond, J. Holyoake, R.W. Hawtin, M.S. Sansom, J. R. Soc., Interface, vol. 5, 2008, pp. S241.

[42] M. Wilhelm, A. Mukherjee, B. Bouvier, K. Zakrzewska, J.T. Hynes, R. Lavery, Journal of the American Chemical Society, vol. 134, American Chemical Society, 2012, pp. 8588-8596.

[43] S. Khalid, M.J. Hannon, A. Rodger, P.M. Rodger, Chemistry – A European Journal, vol. 12, WILEY-VCH Verlag, 2006, pp. 3493-3506.

[44] Y.-Y. Fang, K.B. Lipkowitz, E.C. Long, Journal of Chemical Theory and Computation, vol. 2, American Chemical Society, 2006, pp. 1453-1463.

[45] A. Biancardi, A. Burgalassi, A. Terenzi, A. Spinello, G. Barone, T. Biver, B. Mennucci, Chemistry – A European Journal, vol. 20, WILEY-VCH Verlag, 2014, pp. 7439-7447.

[46] J. Kujawski, K. Czaja, M. Doskocz, M.K. Bernard, B. Drabińska, J. Kruk, A. Myka, Computational and Theoretical Chemistry, vol. 1059, 2015, pp. 45-50.

[47] A. Biancardi, T. Biver, F. Secco, B. Mennucci, Physical Chemistry Chemical Physics, vol. 15, The Royal Society of Chemistry, 2013, pp. 4596-4603.

[48] D. Ambrosek, P.-F. Loos, X. Assfeld, C. Daniel, Journal of Inorganic Biochemistry, vol. 104, 2010, pp. 893-901.

[49] Z. Cimerman, N. Galešić, B. Bosner, Journal of Molecular Structure, vol. 274, 1992, pp. 131-144.

[50] O. Atakol, H. Nazir, M.N. Tahir, Uuml, Lk, Uuml, Din, ccedil, er, Analytical Sciences, vol. 13, 1997, pp. 519-520.

[51] S. Demir, H. Yılmaz, M. Dilimulati, M. Andac, Spectrochimica Acta Part A: Molecular and Biomolecular Spectroscopy, vol. 150, 2015, pp. 523-532.

[52] S. Demir, H. Yilmaz, M. Dilimulati, M. Andaç, Journal of Molecular Modeling, vol. 20, Springer Berlin Heidelberg, 2014, pp. 1-7.

[53] M. Asadi, Z. Asadi, S. Torabi, N. Lotfi, Spectrochimica Acta Part A: Molecular and Biomolecular Spectroscopy, vol. 94, 2012, pp. 372-377.

[54] G. Sheldrick, Acta Crystallographica Section A, vol. 64, 2008, pp. 112-122.

[55] G.M. Sheldrick, 1997.

[56] M.J. Frisch, G.W. Trucks, H.B. Schlegel, G.E. Scuseria, M.A. Robb, J.R. Cheeseman, G. Scalmani, V. Barone, B. Mennucci, G.A. Petersson, H. Nakatsuji, M. Caricato, X. Li, H.P. Hratchian, A.F. Izmaylov, J. Bloino, G. Zheng, J.L. Sonnenberg, M. Hada, M. Ehara, K. Toyota, R. Fukuda, J. Hasegawa, M. Ishida, T. Nakajima, Y. Honda, O. Kitao, H. Nakai, T. Vreven, J.A. Montgomery Jr., J.E. Peralta, F. Ogliaro, M.J. Bearpark, J. Heyd, E.N. Brothers, K.N. Kudin, V.N. Staroverov, R. Kobayashi, J. Normand, K. Raghavachari, A.P. Rendell, J.C. Burant, S.S. Iyengar, J. Tomasi, M. Cossi, N. Rega, N.J. Millam, M. Klene, J.E. Knox, J.B. Cross, V. Bakken, C. Adamo, J. Jaramillo, R. Gomperts, R.E. Stratmann, O. Yazyev, A.J. Austin, R. Cammi, C. Pomelli, J.W. Ochterski, R.L. Martin, K. Morokuma, V.G. Zakrzewski, G.A. Voth, P. Salvador, J.J. Dannenberg, S. Dapprich, A.D. Daniels, Ö. Farkas, J.B. Foresman, J.V. Ortiz, J. Cioslowski, D.J. Fox, Gaussian, Inc., Wallingford, CT, USA, 2013.

[57] G. Felsenfeld, S.Z. Hirschman, Journal of Molecular Biology, vol. 13, 1965, pp. 407-427.

[58] J. Ravichandran, P. Gurumoorthy, M.A. Imran Musthafa, A. Kalilur Rahiman, Spectrochimica Acta Part A: Molecular and Biomolecular Spectroscopy, vol. 133, 2014, pp. 785-793.

[59] D. Řeha, M. Kabeláč, F. Ryjáček, J. Šponer, J.E. Šponer, M. Elstner, S. Suhai, P. Hobza, Journal of the American Chemical Society, vol. 124, American Chemical Society, 2002, pp. 3366-3376.

[60] T. Kubař, M. Hanus, F. Ryjáček, P. Hobza, Chemistry – A European Journal, vol. 12, WILEY-VCH Verlag, 2006, pp. 280-290.

[61] P. Hobza, J. Sponer, M. Polasek, Journal of the American Chemical Society, vol. 117, American Chemical Society, 1995, pp. 792-798.

[62] J. Šponer, J. Leszczyński, P. Hobza, The Journal of Physical Chemistry, vol. 100, American Chemical Society, 1996, pp. 5590-5596.

[63] Y. Zhao, D.G. Truhlar, n. null, J Phys Chem A, vol. 110, 2006, pp. 5121.

[64] Y. Zhao, D.G. Truhlar, Theor. Chem. Acc., vol. 120, 2008, pp. 215.

[65] M. Swart, T. van der Wijst, C. Fonseca Guerra, F.M. Bickelhaupt, Journal of Molecular Modeling, vol. 13, Springer-Verlag, 2007, pp. 1245-1257.

[66] A. Robertazzi, A. Magistrato, P. de Hoog, P. Carloni, J. Reedijk, Inorganic Chemistry, vol. 46, American Chemical Society, 2007, pp. 5873-5881.

[67] G. Barone, C.F. Guerra, N. Gambino, A. Silvestri, A. Lauria, A.M. Almerico, F.M. Bickelhaupt, Journal of Biomolecular Structure and Dynamics, vol. 26, Taylor & Francis, 2008, pp. 115-129.

[68] V. Dryza, E.J. Bieske, Int. J. Mass Spectrom., vol. 297, 2010, pp. 46.

[69] G. Altinay, M. Citir, R.B. Metz, J. Phys. Chem. A, vol. 114, 2010, pp. 5104.

[70] A. Kocak, Z. Sallese, M.D. Johnston, R.B. Metz, The Journal of Physical Chemistry A, vol. 118, American Chemical Society, 2014, pp. 3253-3265.

[71] A. Kocak, G. Austein-Miller, W.L. Pearson, G. Altinay, R.B. Metz, The Journal of Physical Chemistry A, vol. 117, American Chemical Society, 2013, pp. 1254-1264.

[72] A. Kocak, G. Austein-Miller, W.L. Pearson, G. Altinay, R.B. Metz, J. Phys. Chem. A, vol. 117, 2012, pp. 1254.

[73] A. Kocak, Depaetment of Chemistry, vol. PhD, University of Massachusetts Amherst, Amherst, MA, 2014.

[74] A. Silvestri, G. Barone, G. Ruisi, D. Anselmo, S. Riela, V.T. Liveri, Journal of Inorganic Biochemistry, vol. 101, 2007, pp. 841-848.

[75] N.H. Campbell, N.H.A. Karim, G.N. Parkinson, M. Gunaratnam, V. Petrucci, A.K. Todd, R. Vilar, S. Neidle, Journal of Medicinal Chemistry, vol. 55, American Chemical Society, 2012, pp. 209-222.

[76] R.L. Martin, J. Chem. Phys., vol. 118, 2003, pp. 4775.

[77] M.T. Carter, M. Rodriguez, A.J. Bard, Journal of the American Chemical Society, vol. 111, American Chemical Society, 1989, pp. 8901-8911.

[78] D.E.V. Schmechel, D.M. Crothers, Biopolymers, vol. 10, Wiley Subscription Services, Inc., A Wiley Company, 1971, pp. 465-480.

[79] T.-C. Tang, H.-J. Huang, Electroanalysis, vol. 11, VCH Verlagsgesellschaft mbH, 1999, pp. 1185-1190.

[80] J.B. Lepecq, C. Paoletti, Journal of Molecular Biology, vol. 27, 1967, pp. 87-106.

[81] M. Hossain, P. Giri, G.S. Kumar, DNA & Cell Biology, vol. 27, Mary Ann Liebert, Inc., 2008, pp. 81-90.

[82] C. Tong, Z. Hu, J. Wu, Journal of Fluorescence, vol. 20, Springer US, 2010, pp. 261-267.

[83] L.S. Lerman, J. Mol. Biol., vol. 3, 1961, pp. 18.

[84] I. Haq, P. Lincoln, D. Suh, B. Norden, B.Z. Chowdhry, J.B. Chaires, Journal of the American Chemical Society, vol. 117, American Chemical Society, 1995, pp. 4788-4796.

[85] D. Suh, J.B. Chaires, Bioorganic & Medicinal Chemistry, vol. 3, 1995, pp. 723-728.

[86] G. Cohen, H. Eisenberg, Biopolymers, vol. 8, Wiley Subscription Services, Inc., A Wiley Company, 1969, pp. 45-55.

Square planar Cu(II) complex of salphen type Schiff base, N,N'-disalicylidene-2,3-diaminopyridine, was synthesized, characterized and analyzed for its intercalative binding to a double stranded DNA both experimentally and theoretically. Both suggested strong intercalation.